Supplemental Information

Cognitive strategies shift information from single neurons to populations in prefrontal cortex

Feng-Kuei Chiang, Joni D. Wallis, & Erin L. Rich

Cognitive strategies shift information from single neurons to populations in prefrontal cortex

Feng-Kuei Chiang, Joni D. Wallis, & Erin L. Rich

Subject R								
Recording sessions	Electrodes Left / Right	Recorded units	Stereotyped index					
			block#1	block#2	block#3	block#4	block#5	block#6
#1	12 / 12	27	0.061	0.117	0.000	-0.325	-0.061	-0.162
#2	16 / 16	72	0.008	0.075	-0.378	-0.175	-0.026	-0.075
#3	16 / 16	48	0.317	-0.242	0.125	0.108	0.018	-0.248
#4	16 / 16	57	0.103	0.316	0.042	0.009	-0.167	0.061
#5	16 / 16	39	0.044	0.070	-0.150	0.263	-0.188	-0.257
#6	16 / 16	43	-0.324	-0.308	0.282	-0.026	-0.208	-0.234
#7	16 / 16	51	0.425	0.043	-0.018	0.158	-0.085	-0.451
#8	16 / 16	42	-0.308	-0.436	0.265	-0.256	-0.333	0.105
#9	16 / 16	41	0.385	0.036	0.291	-0.287	0.145	-0.283
#10	16 / 16	56	0.034	0.242	0.283	-0.083	0.202	-0.036
#11	16 / 16	54	-0.308	-0.053	-0.009	-0.296	0.167	0.017
#12	16 / 16	53	0.077	0.150	0.019	-0.102	-0.225	-0.241
#13	16 / 16	46	-0.342	-0.050	-0.067	-0.083	-0.017	-0.090
#14	16 / 16	39	0.162	0.192	0.430	-0.308	-0.017	-0.128
#15	16 / 16	41	-0.042	0.142	-0.070	-0.298	-0.425	-0.267
	subtotal	709						

Subject Q								
Recording sessions	Electrodes Left / Right	Recorded units	Stereotyped index					
			block#1	block#2	block#3	block#4	block#5	block#6
#1	16 / 16	28	-0.137	0.298	0.099	-0.102	-0.059	-0.034
#2	16 / 16	37	-0.282	-0.143	-0.200	0.062	-0.310	[redacted]
#3	16 / 16	25	0.387	-0.552	0.152	-0.086	-0.310	0.351
#4	16 / 16	43	0.325	0.124	-0.299	-0.417	0.200	-0.200
#5	16 / 16	30	-0.036	-0.117	0.126	-0.250	0.323	-0.137
#6	12 / 16	38	0.350	0.017	0.083	0.018	0.009	0.189
#7	12 / 16	40	-0.154	0.299	-0.279	0.108	0.027	0.063
#8	12 / 16	40	0.183	0.569	0.297	-0.028	-0.361	-0.167
#9	12 / 16	44	0.400	-0.175	-0.065	0.324	0.009	0.045
#10	12 / 16	43	0.342	0.269	0.135	-0.069	-0.162	0.028
	subtotal	368						

Supplemental Table S1. Related to STAR Methods. Details of single-unit recordings across sessions. Numbers of electrodes, recorded units, and calculated SIs in each block were listed across recording sessions. The blacked-out block was excluded from further analysis because there were less than 20 completed trials. There was no evidence of changes in SI across sessions. A GLM predicted SI from block number, session number, and block x session interaction, and found no main effects of session or interaction ($p > 0.05$ in both subjects). There was a reduction in stereotyped behavior across blocks within a session in subject R only ($p < 0.01$; subject Q, $p > 0.05$).

Task variables	X	Y	Radius	Saccade order	SI	X-1	Y-1	X+1	Y+1	Color
Subject R										
proportion of selective neurons	0.55	0.41	0.26	0.21	0.22	0.06	0.08	0.04	0.09	0.02
Session correlation	0.01	0.08	0.08	-0.05	-0.03	0.06	0.17	-0.40	0.00	-0.11
p value	0.77	0.15	0.27	0.53	0.68	0.73	0.20	0.03	0.99	0.68
Subject Q										
proportion of selective neurons	0.33	0.25	0.19	0.08	0.20	0.04	0.03	0.04	0.05	0.02
Session correlation	-0.06	-0.32	0.21	-0.01	0.00	0.07	0.23	0.08	0.29	-0.20
p value	0.48	0.00	0.08	0.94	1.00	0.80	0.47	0.80	0.26	0.61

Supplemental Table S2. Related to Figure2. Task variables encoded by single units. We used general linear models to predict each neuron's firing rate during the hold target epoch from 10 regressors. The top row shows the proportion of recorded neuron that significantly encodes each variable. A neuron was considered to encode a variable if the associated beta coefficient was significantly non-zero ($p < 0.01$). The analysis is similar to that in Chiang and Wallis (2018b), but includes additional task variables. To test for changes in task coding across sessions, we correlated the beta coefficients with session number. The second and third lines show the corresponding r and p-values. There was one significant trend per subject (red), but these were inconsistent across subjects and one was only marginally significant, indicating no strong evidence that neural coding changes across sessions in this task. X = x-position of current target, Y = y-position of current target, Radius = distance to current target, Saccades = position in sequence, SI = SI of the block, X-1 = x-position of previous target, Y-1 = y-position of previous target, X+1 = x-position of next target, Y+1 = y-position of next target, Color = target color for the trial.

Target location decoder				
Subject R	X_coordinate	Y_coordinate	Saccade order	Stereotyped index
correlation coefficient =	-0.055	0.004	0.008	0.014
p-value =	4.3 x 10e-15 ***	0.533	0.253	4.1 x 10e-02 *
Subject Q	X_coordinate	Y_coordinate	Saccade order	Stereotyped index
correlation coefficient =	0.037	0.033	0.011	0.048
p-value =	3.42 x 10e-05 ***	2.6 x 10e-04 ***	0.223	1.0 x 10e-07 ***

Saccade order decoder				
Subject R	X_coordinate	Y_coordinate	Saccade order	Stereotyped index
correlation coefficient =	0.006	0.01	-0.065	-0.012
p-value =	0.400	0.135	5.58 x 10e-21 ***	0.083
Subject Q	X_coordinate	Y_coordinate	Saccade order	Stereotyped index
correlation coefficient =	-0.017	-0.008	-0.074	0.005
p-value =	0.064	0.352	9.21 x 10e-17 ***	0.587

Supplemental Table S3. Related to Figure 3. Partial correlation statistics between task variables and decoders. Target locations and selection orders had mutually exclusive influences on decoding performances of target location and saccade order decoders. We used partial correlations to further examine the extent to which decoding performance was affected by correlations between target locations and saccade orders. For each response, decoding performance was quantified by the posterior probability of the correct classification (e.g. target selections or saccade orders) as calculated by LDA. Two partial correlations were then conducted between decoding performance (for target location or saccade order decoder) and four task variables: locations (target X- or Y-coordinates), sequence (saccade order), and strategy (stereotyped index, SI). Therefore, the analysis reveals the effect of each factor on decoding performance, while controlling for the other three. The table summarizes partial correlation coefficients and p values for each analysis. Asterisks indicate statistical significance level, *$p < 0.05$ and ***$p < 0.001$. The target location decoder was affected by X and Y positions, meaning that some areas of the screen were better decoded than others. It was also affected by SI, with a positive correlation coefficient, indicating better location decoding with more stereotyped behavior, after controlling for all other variables. In contrast, the saccade order decoder was affected by the saccade number, meaning some saccades were better decoded than others. This decoder’s performance was not significantly affected by SI, suggesting that correlations between saccade order and target location accounted for the improvement in saccade order decoding. Taken together, these results indicate significant improvements in target decoding with more stereotyped behaviors that cannot be accounted for by changes in the order of target selection.

Target Location

Subject R

	Positive Noise Correlations						Negative Noise Correlations					
	A	B	C	D	E	F	A	B	C	D	E	F
Early Fixation	r = -0.09 p = 0.41	r = -0.15 p = 0.15	r = -0.03 p = 0.77	r = -0.22 p = 0.04	r = -0.02 p = 0.83	r = -0.16 p = 0.14	r = 0.03 p = 0.79	r = -0.09 p = 0.41	r = 0.01 p = 0.90	r = 0.20 p = 0.06	r = -0.04 p = 0.68	r = 0.09 p = 0.38
Late Fixation	r = -0.18 p = 0.08	r = -0.08 p = 0.48	r = -0.07 p = 0.54	r = -0.13 p = 0.21	r = -0.03 p = 0.81	r = 0.65 p = 0.54	r = 0.03 p = 0.82	r = 0.27 p = 0.01	r = -0.10 p = 0.35	r = 0.28 p = 0.008	r = -0.15 p = 0.16	r = 0.19 p = 0.07
Hold Target	r = -0.38 p = 0.72	r > -0.01 p = 0.97	r = -0.05 p = 0.67	r = -0.15 p = 0.15	r > -0.01 p = 0.96	r = -0.11 p = 0.32	r = 0.03 p = 0.80	r = -0.08 p = 0.47	r = 0.11 p = 0.32	r = 0.23 p = 0.03	r = -0.05 p = 0.53	r = 0.12 p = 0.25
Reward	r = -0.08 p = 0.46	r = -0.02 p = 0.88	r = -0.15 p = 0.17	r = -0.07 p = 0.54	r = -0.09 p = 0.40	r = -0.13 p = 0.24	r = 0.13 p = 0.21	r = 0.05 p = 0.66	r = 0.03 p = 0.80	r = -0.18 p = 0.09	r = -0.02 p = 0.87	r = -0.07 p = 0.45

Subject Q

	Positive Noise Correlations						Negative Noise Correlations					
	A	B	C	D	E	F	A	B	C	D	E	F
Early Fixation	r = -0.15 p = 0.27	r < 0.01 p = 0.99	r = -0.02 p = 0.91	r = -0.02 p = 0.88	r = -0.06 p = 0.63	r = -0.05 p = 0.73	r < 0.01 p = 0.96	r = 0.08 p = 0.55	r = 0.32 p = 0.01	r = -0.01 p = 0.92	r = 0.07 p = 0.59	r = 0.36 p = 0.005
Late Fixation	r = -0.06 p = 0.66	r = -0.04 p = 0.74	r < 0.01 p = 0.97	r = 0.10 p = 0.44	r > -0.01 p = 0.95	r = -0.15 p = 0.25	r = 0.05 p = 0.69	r = 0.06 p = 0.65	r = -0.15 p = 0.25	r = 0.12 p = 0.36	r = 0.03 p = 0.80	r = 0.09 p = 0.50
Hold Target	r = 0.01 p = 0.94	r = 0.17 p = 0.21	r > -0.01 p = 0.95	r = -0.05 p = 0.73	r = -0.03 p = 0.81	r = 0.06 p = 0.66	r = -0.05 p = 0.72	r = -0.08 p = 0.55	r > -0.01 p = 1.00	r = -0.08 p = 0.55	r = 0.11 p = 0.42	r = -0.05 p = 0.70
Reward	r = 0.06 p = 0.66	r = 0.19 p = 0.15	r = 0.14 p = 0.30	r = 0.06 p = 0.69	r = 0.28 p = 0.03	r = -0.04 p = 0.78	r = -0.03 p = 0.84	r = 0.16 p = 0.22	r = -0.12 p = 0.38	r = 0.21 p = 0.11	r = -0.08 p = 0.55	r = -0.11 p = 0.43

Saccade Order

Subject R

	Positive Noise Correlations						Negative Noise Correlations					
	1	2	3	4	5	6	1	2	3	4	5	6
Early Fixation	r = -0.21 p = 0.05	r = -0.08 p = 0.48	r = -0.04 p = 0.72	r = -0.16 p = 0.12	r = -0.04 p = 0.71	r = -0.02 p = 0.84	r = -0.08 p = 0.43	r = 0.07 p = 0.55	r = 0.03 p = 0.80	r = -0.01 p = 0.92	r > -0.01 p = 0.94	r = 0.24 p = 0.03
Late Fixation	r = -0.19 p = 0.07	r = 0.02 p = 0.83	r < 0.01 p = 0.97	r > -0.01 p = 0.93	r = 0.05 p = 0.66	r = -0.05 p = 0.65	r = -0.04 p = 0.73	r = -0.14 p = 0.20	r = 0.11 p = 0.33	r = -0.06 p = 0.56	r = 0.04 p = 0.69	r = -0.05 p = 0.68
Hold Target	r = -0.24 p = 0.02	r = -0.03 p = 0.76	r = -0.18 p = 0.09	r = 0.06 p = 0.59	r = -0.03 p = 0.78	r = 0.08 p = 0.46	r = -0.16 p = 0.13	r = 0.06 p = 0.57	r = -0.04 p = 0.70	r > -0.01 p = 0.95	r = 0.07 p = 0.51	r = 0.14 p = 0.18
Reward	r = -0.02 p = 0.83	r = -0.06 p = 0.58	r = -0.02 p = 0.88	r = -0.14 p = 0.18	r = -0.12 p = 0.25	r = -0.06 p = 0.58	r = -0.13 p = 0.23	r > -0.01 p = 0.96	r = -0.06 p = 0.55	r = -0.01 p = 0.92	r = -0.03 p = 0.77	r = -0.07 p = 0.51

Subject Q

	Positive Noise Correlations						Negative Noise Correlations					
	1	2	3	4	5	6	1	2	3	4	5	6
Early Fixation	r = 0.01 p = 0.92	r = -0.06 p = 0.67	r > -0.01 p = 0.96	r = -0.03 p = 0.82	r = -0.09 p = 0.52	r = -0.06 p = 0.63	r = 0.08 p = 0.53	r = 0.11 p = 0.42	r = -0.05 p = 0.73	r = 0.19 p = 0.16	r = 0.19 p = 0.15	r < 0.01 p = 0.99
Late Fixation	r = 0.21 p = 0.10	r = 0.17 p = 0.20	r = -0.01 p = 0.94	r = -0.11 p = 0.42	r = 0.13 p = 0.34	r = -0.12 p = 0.36	r = 0.05 p = 0.70	r = 0.23 p = 0.08	r = 0.03 p = 0.80	r = 0.28 p = 0.03	r = -0.04 p = 0.79	r = 0.03 p = 0.82
Hold Target	r = 0.02 p = 0.86	r = 0.02 p = 0.86	r = -0.09 p = 0.50	r = 0.18 p = 0.16	r = 0.04 p = 0.74	r = 0.03 p = 0.84	r = -0.10 p = 0.46	r = -0.07 p = 0.63	r = 0.06 p = 0.65	r = 0.07 p = 0.59	r = -0.08 p = 0.57	r = 0.05 p = 0.72
Reward	r = 0.06 p = 0.68	r = -0.22 p = 0.09	r = 0.08 p = 0.56	r = 0.06 p = 0.66	r = 0.14 p = 0.29	r = 0.04 p = 0.78	r = 0.18 p = 0.18	r = -0.04 p = 0.77	r > -0.01 p = 0.97	r = 0.08 p = 0.56	r = -0.03 p = 0.80	r = 0.11 p = 0.39

Supplemental Table S4. Related to Figure 3. Noise correlation tables. We analyzed how the proportion of neurons with correlated variability across target locations (top) and saccade sequence position (bottom) changed with SI. Values are reported for the Pearson correlation between proportion of neuron pairs with significant positive / negative correlated activity versus SI. Uncorrected r and p-values are shown for all contrasts related to each target selected (A to F) or saccade executed (1 to 6). Rows show the same measures in different epochs.

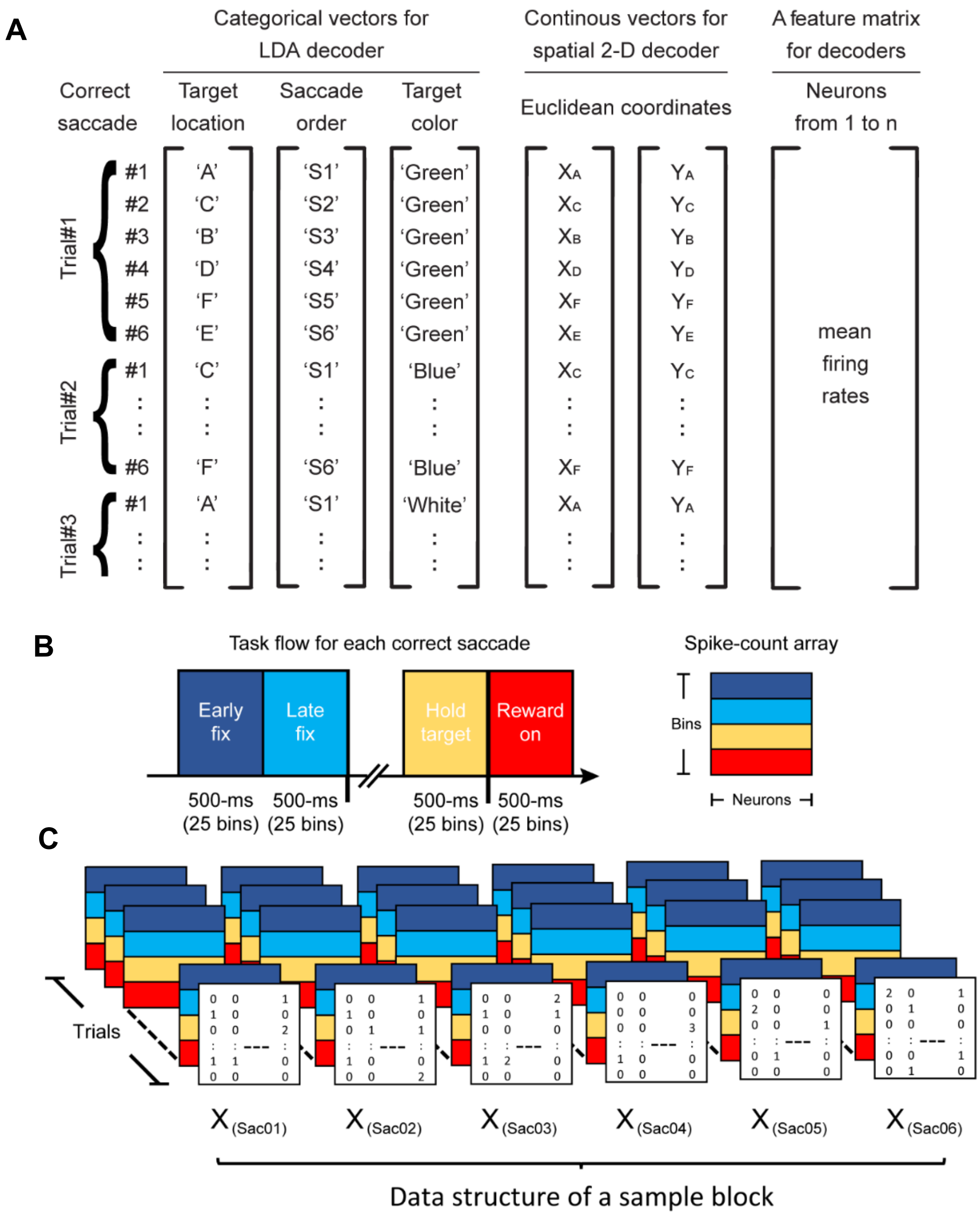

Supplemental Figure S1. Related to STAR Methods. Data structures used for analyses. (A) Decoding structures. Three categorical decoders were separately trained and tested to classify target locations, saccade orders, and target colors. Labels for the target location decoder were 6 categories corresponding to each of the 6 targets (target A, B, etc.), labels for the saccade order decoder were 6 ordered saccade responses (saccade#1, #2, etc.), and labels for the target color decoder were three colors (green, blue, and white). For 2D spatial decoding, ridge regressions separately predicted target X- or Y-coordinates. The feature matrix was the same for all decoders, and consisted of mean firing rates of each neuron (1 to n) in columns and each correct saccade in rows. Mean firing rates were calculated for a given epoch, or in sliding windows (see Methods). (B-C) Schematic of the data structures used for the dimensionality analyses. (B) Four 500ms epochs in each complete trial were each separated into 25 non-overlapping 20ms bins for each neuron to create spike-count arrays. (C) The data structure for each target selection ($X_{(sac\#)}$) included the spike-count arrays arranged by trials and saccade orders.

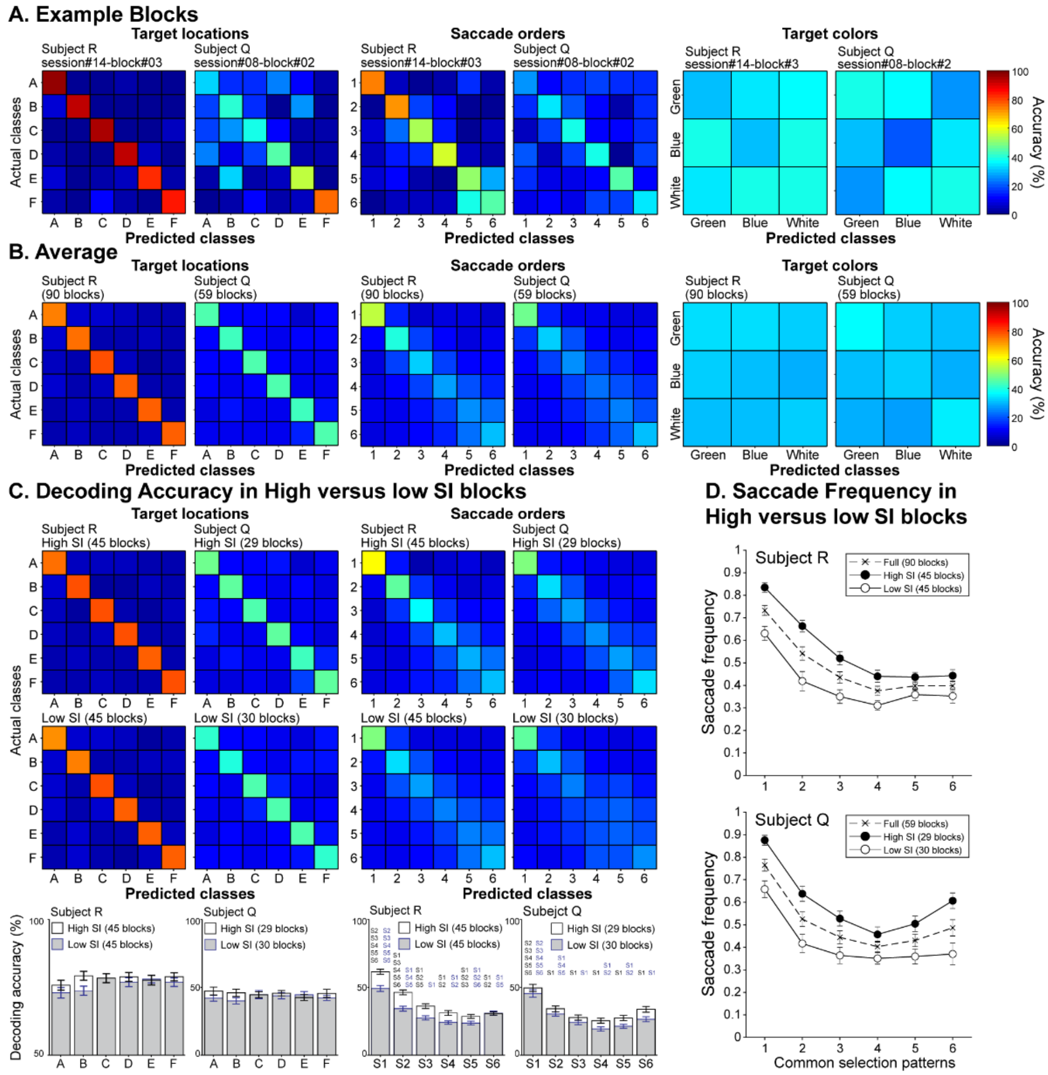

Supplemental Figure S2. Related to Figure 3. Confusion matrices of decoding performance during the hold target epoch. (A) Target location, saccade order, and target color decoders in an example block from each subject. (B) Average decoding across all blocks from each subject. The colormap indicates average decoding accuracies of each predicted class compared to the actual class. The mean decoding accuracy used as a measure of decoder performance was calculated by taking the mean values on the diagonal, which indicate how well actual classes were predicted. Chance levels of decoding are 16.6% for target location and saccade order, and 33.3% for target color decoder. (C) Average decoding for high and low SI blocks. Bar plots are data from the main diagonals, error bars = SEM. [ANOVAs: Target locations: SI block, subject R: $F_{(1,528)} = 4.26$, $p = 0.04$, Q: $F_{(1,342)} = 2.94$, $p = 0.09$; Saccade position, subject R: $F_{(5,528)} = 1.56$, $p = 0.17$, Q: $F_{(5,342)} = 0.18$, $p = 0.97$; interaction, subject R: $F_{(5,528)} = 0.8$, $p = 0.55$, Q: $F_{(5,342)} = 0.83$, $p = 0.53$. Saccade order: SI block, subject R: $F_{(1,528)} = 60.67$, $p = 3.60 \times 10^{-14}$, Q: $F_{(1,342)} = 20.2$, $p = 9.54 \times 10^{-6}$; Saccade position: subject R: $F_{(5,528)} = 86.9$, $p = 1.43 \times 10^{-66}$, Q: $F_{(5,342)} = 42.33$, $p = 6.87 \times 10^{-34}$; interaction, subject R: $F_{(5,342)} = 0.83$, $p = 0.53$, Q: $F_{(5,342)} = 0.3$, $p = 0.92$]. Notations show which saccades each bar significantly differs from on post-hoc tests. (D) Rate of following common selection order at each sequence position. The common order was followed more frequently on HSI blocks (filled circles) for all 6 selections. There was a tendency to follow the pattern more on early targets, and this increased in high SI blocks (ANOVAs: H/LSI x target number interaction R: $F_{(5,528)} = 5.59$, $p = 4.91 \times 10^{-5}$, Q: $F_{(5,342)} = 2.22$, $p = 0.05$), but HSI and LSI blocks are distinct throughout all 6 targets, so high SI's aren't driven exclusively by first or last target effects. Dashed line = both groups pooled together for reference. Error bars = SEM.

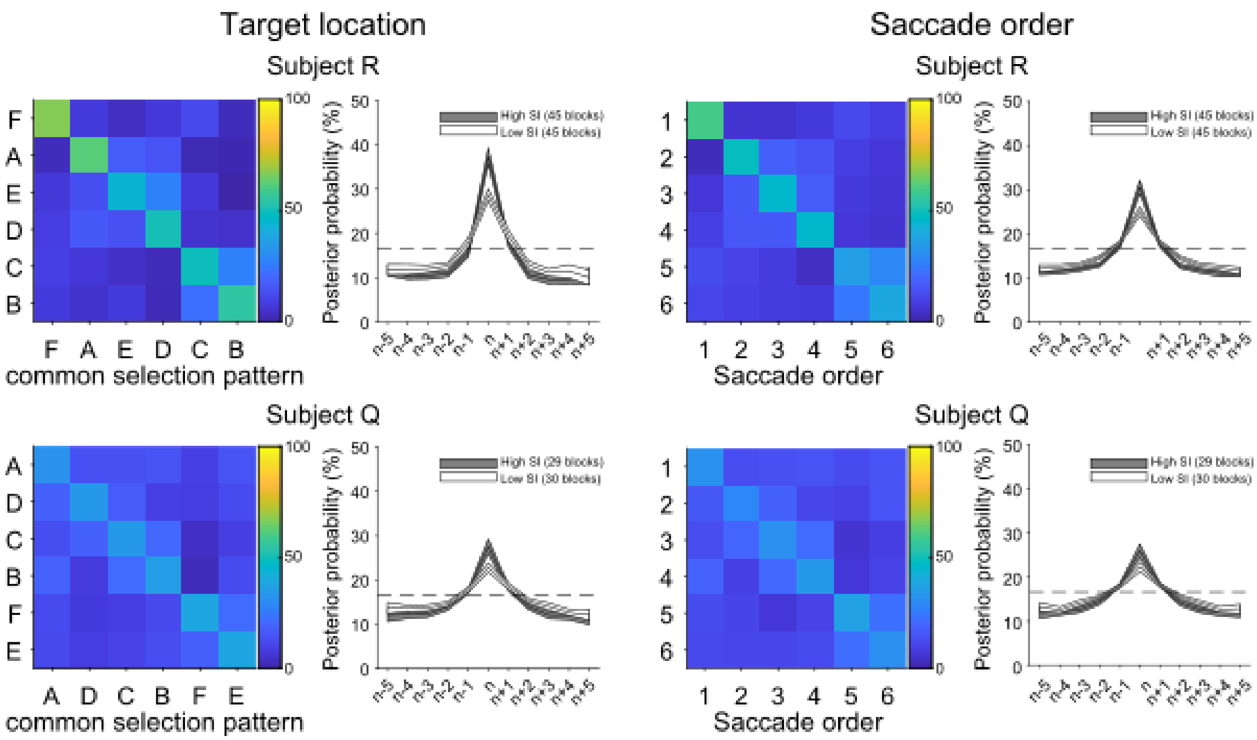

Supplemental Figure S3. Related to Figure 3. Decoding of past and future targets. Posterior probabilities from the target location and saccade order decoders, re-ordered relative to each saccade in a sequence (n), and separated into high and low SI blocks. There were higher probabilities (better decoding) for the current target and these were higher on high SI blocks (t-tests on position n only, $p < 0.0001$ for all). In all cases, there are slightly higher probabilities on n-1 and n+1 saccades, suggesting some representation of past and future targets (see Chiang and Wallis, 2018b), but these effects do not change with SI. Two-way ANOVAs found significant effects of relative position and high/low SI, and their interaction in each data set, but this was driven only by saccade n (post-hoc $p < 0.01$ at saccade n for each), indicating that more distributed coding we find in high SI blocks is not due to increased coding of other targets in the sequence. Note that posterior probabilities are normalized to sum to 1.0, so that the non-current targets that are not coded by the population have probabilities below theoretical chance, which is 1/6, or 16.7% (dashed line). Shading = 95% CI. ANOVA results: Subject R - Target location decoder: SI group $F_{(1,968)} = 4.39$, $p = 0.036$; relative position $F_{(10,968)} = 274.79$, $p = 1.26 \times 10^{-274}$; group x position $F_{(10,968)} = 14.94$, $p = 5.24 \times 10^{-25}$ [interaction]. Subject R - Saccade order decoder: SI group $F_{(1,968)} = 8.43$, $p = 0.004$; relative position $F_{(10,968)} = 389.89$, $p < 0.001$; group x position $F_{(10,968)} = 16.73$, $p = 3.59 \times 10^{-28}$. Subject Q - Target location decoder: SI group $F_{(1,627)} = 8.43$, $p = 0.005$; relative position $F_{(10,627)} = 154.65$, $p = 5.94 \times 10^{-162}$; group x position $F_{(10,627)} = 8.20$, $p = 1.50 \times 10^{-12}$; Subject Q - Saccade order decoder: group $F_{(1,627)} = 6.19$, $p = 0.013$; position $F_{(10,627)} = 167.00$, $p = 1.92 \times 10^{-169}$; group x position $F_{(10,627)} = 6.83$, $p = 3.63 \times 10^{-10}$.

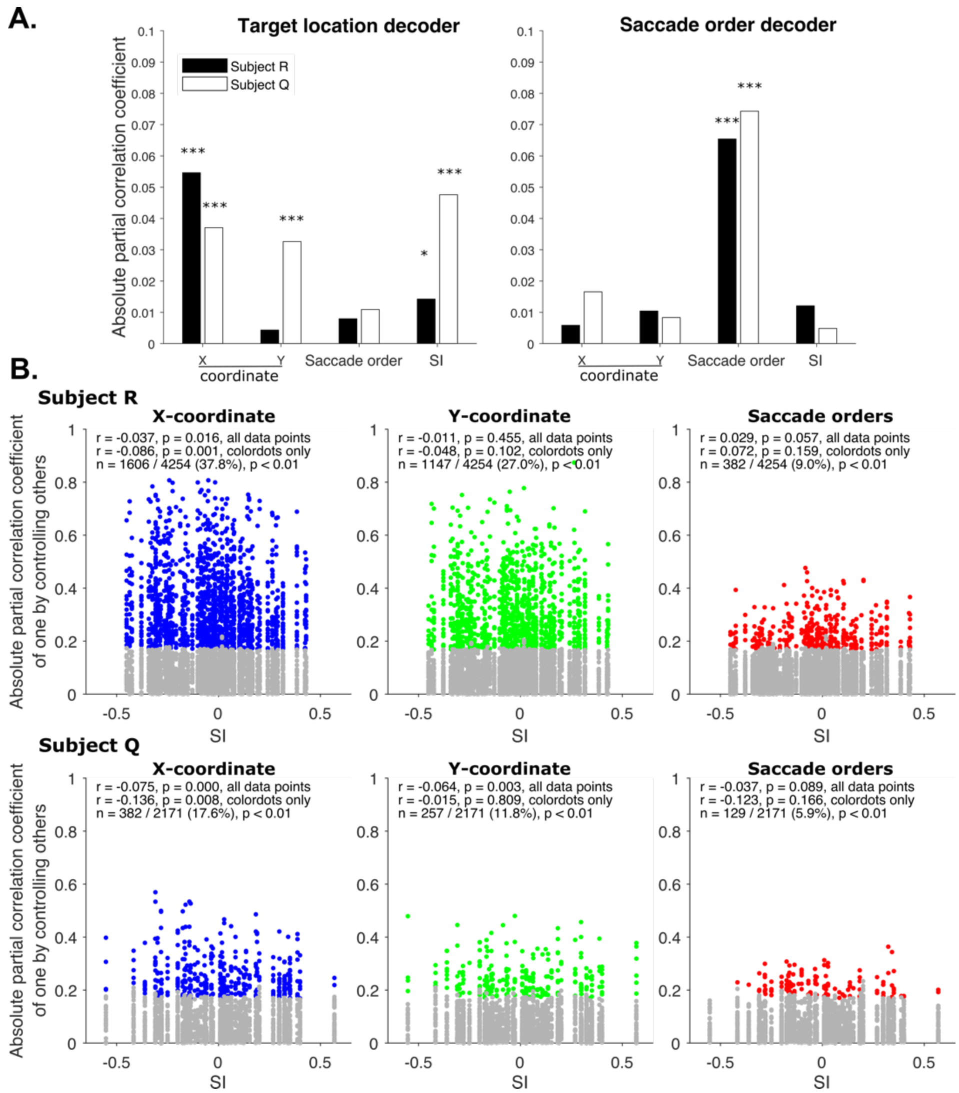

Supplemental Figure S4. Related to Figure 3. Partial correlations between task variables, decoders, and neural activities. (A) Plots of data in Supplemental Table S2, showing two partial correlations: target location or saccade order decoding performance versus four task variables (X-coordinate, Y-coordinate, sequence position, and SI). The target location decoder was affected by spatial coordinates, meaning that some areas of the screen were better decoded than others, and by SI, indicating better location decoding with more stereotyped behavior. Therefore, significant improvements in target decoding with more stereotyped behaviors that cannot be accounted for by changes in the order of target selection. The saccade order decoder was affected by the saccade number, meaning some saccades were better decoded than others, but not SI. *p < 0.05 and ***p < 0.001. (B) Partial correlations between firing rate at the hold target epoch and saccade order (1 to 6), X- and Y-coordinates, plotted against SI for subject R (top) and subject Q (bottom). Each point is a partial correlation coefficient from recorded unit in one trial block (n = 4254, 2171 unit-blocks for subject R, Q). Gray points had no significant partial correlation, indicating that the neurons' mean firing rates did not change with one of three factors (X-coordinate, Y-coordinate, and saccade orders) when controlling the other two. Colored dots show units with significant partial correlations. Assessing changes with increasing SI revealed smaller correlations with X-position in both subjects at higher SIs, indicating less spatial information among single units, when controlling for saccade order.

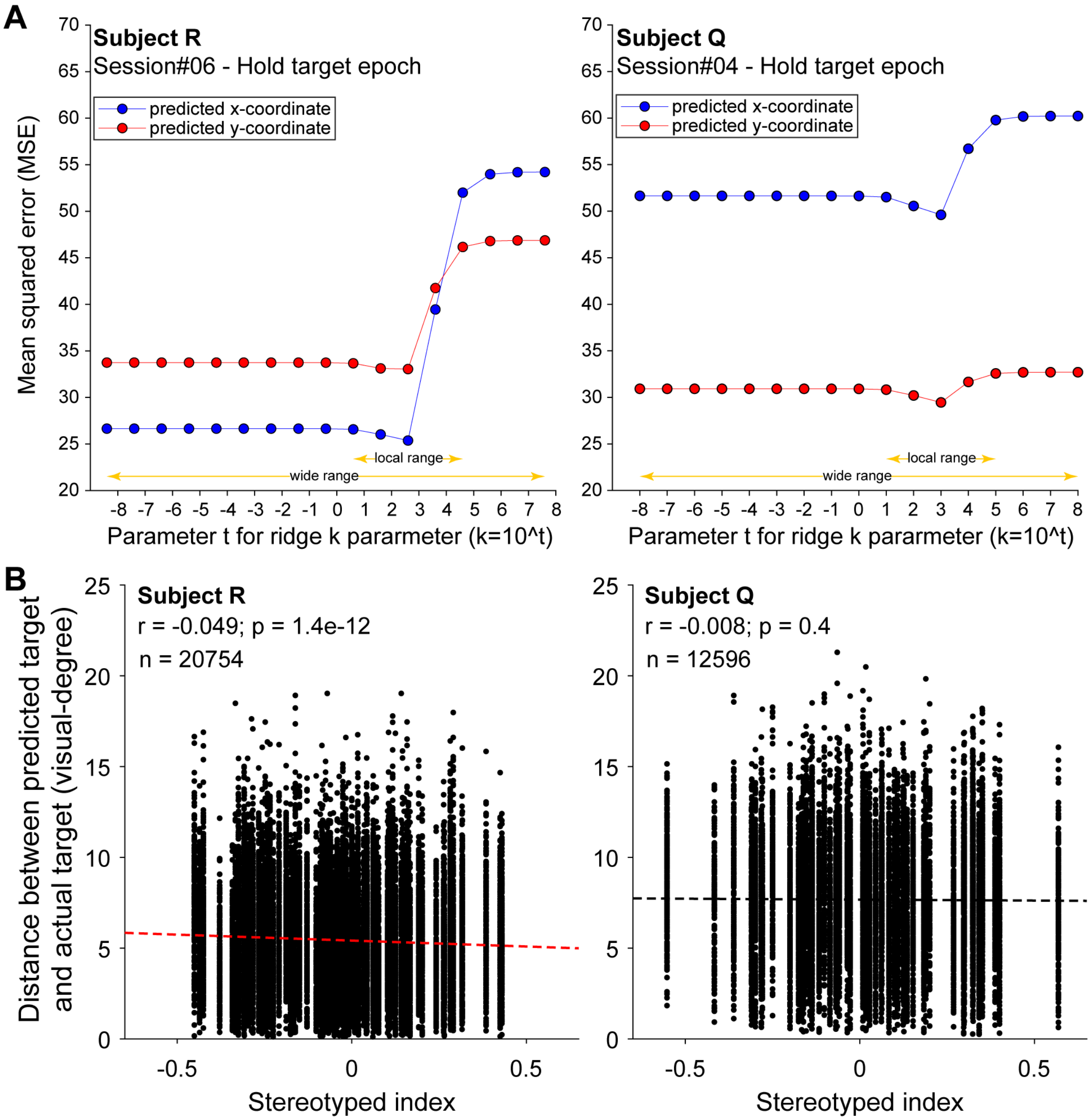

Supplemental Figure S5. Related to Figure 4. Two-dimensional spatial decoding. (A) The optimal ridge regression parameter k was determined by the minimum MSE in two steps. The panels show one example block from each subject, in which the x-axes are the exponents to the base 10 for calculation of parameter k. Parameters were first searched over a wide range, and then a local range was searched around the minimum found in the first step (yellow arrows). (B) Decoding performance was quantified for each target selection as the distance between actual and predicted targets and plotted as a function of SI. Performance improved with SI in subject R and was unaffected subject Q, demonstrating no loss of spatial information at the population level with more stereotyped behaviors. Scatter plots show original data that were binned in Figure 4B.

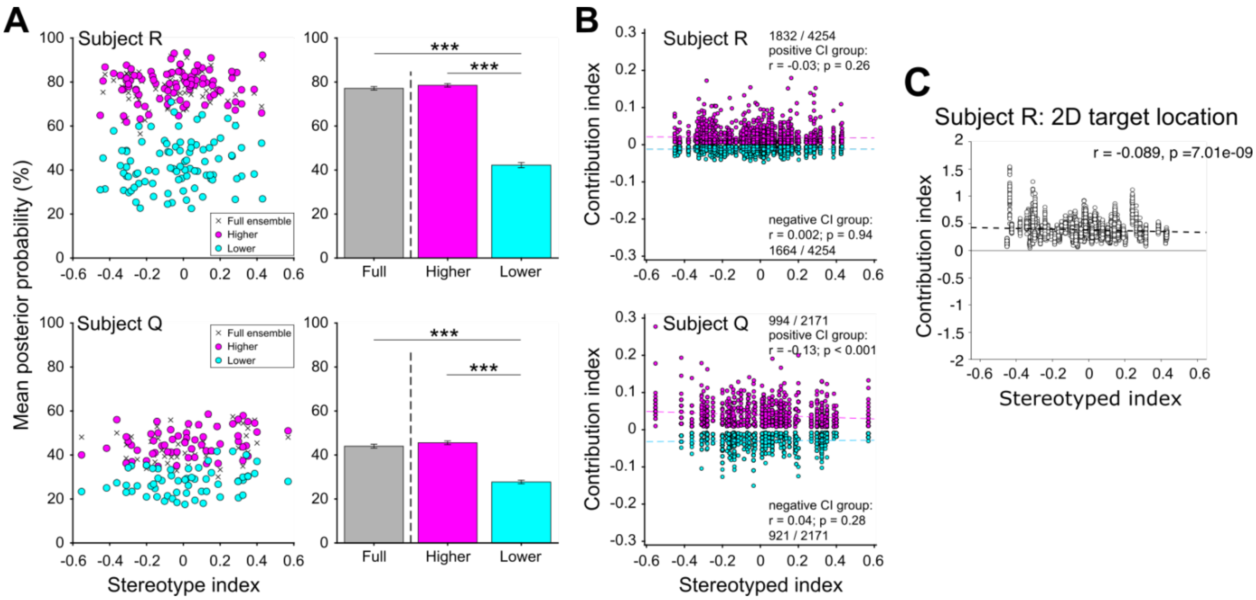

Supplemental Figure S6. Related to Figure 5. Units contributions to the target location decoder. (A) Scatter plots show block-wise mean target location decoding as a function of SI for the full ensemble (+), higher contribution (magenta), and lower contribution (cyan) subgroups. Decoding accuracy corresponds to the proportion of selected targets accurately classified. There were significant main effects between subgroups for both subjects [Two-way ANCOVA, $F_{(1,176)} = 693.3$, $p < 0.001$ for subject R; $F_{(1,114)} = 257.9$, $p < 0.001$ for subject Q], a main effect of SI in one subject [$F_{(1,176)} = 1.65$, $p = 0.20$ for subject R; $F_{(1,114)} = 8.46$, $p < 0.004$ for subject Q], and no interactions [$F_{(1,176)} = 0.71$, $p = 0.40$ for subject R; $F_{(1,114)} = 8.46$, $p = 0.57$ for subject Q]. There were very high decoding accuracies in the subject with no effect of SI, suggesting a ceiling effect. Barplots show the overall means, collapsed across SI. Decoding accuracy from the lower, but not higher contribution group, was significantly worse than from full neural ensemble (Pairwise t-tests, ***p < 0.001). (B) Population data showing CI as a function of SI. Each point is the contribution of one neuron to one block. Neurons making positive contributions (magenta) improved decoder performance, while those making negative contributions (cyan) reduced it. There was a significant SI x contribution type interaction in predicting contribution indices in subject Q [Two-way ANCOVA: $F_{(1, 3492)} = 1.11$, $p = 0.29$, for subject R; $F_{(1,1911)} = 14.68$, $p < 0.001$, for subject Q]. Post-hoc comparisons found that the positive contribution group was negatively correlated with SI, but the negative contribution group had no correlation. [n = 1832, 994 positive, 1664, 921 negative out of 4254, 2171 neurons for subject R, Q; Pearson correlations, positive CI: $r = -0.026$, $p = 0.26$ for subject R; $r = -0.13$, $p < 0.001$ for subject Q; negative CI: $r = 0.002$, $p = 0.94$ for subject R; $r = 0.04$, $p = 0.28$ for subject Q]. (C) Target location decoding in subject R did not reveal significant effects similar to subject Q or saccade order decoding, but decoder performance was very high for this subject (panels A-B), leading to the possibility that ceiling effects limited our ability to assess information content in single units. Therefore, we computed CIs using the 2D spatial decoder described for Figure 4. Accuracy was quantified as the Euclidian distance between actual and predicted targets, and CI was calculated as previously described. This approach decodes different task information (X and Y coordinates), using a different algorithm (regularized regression), and indeed found a different pattern of contributions, where no units made negative contributions across an entire block. Nonetheless, CIs consistently decreased with SI, similar to the other approaches [$r = -0.09$, $p = 7.01 \times 10^{-9}$].

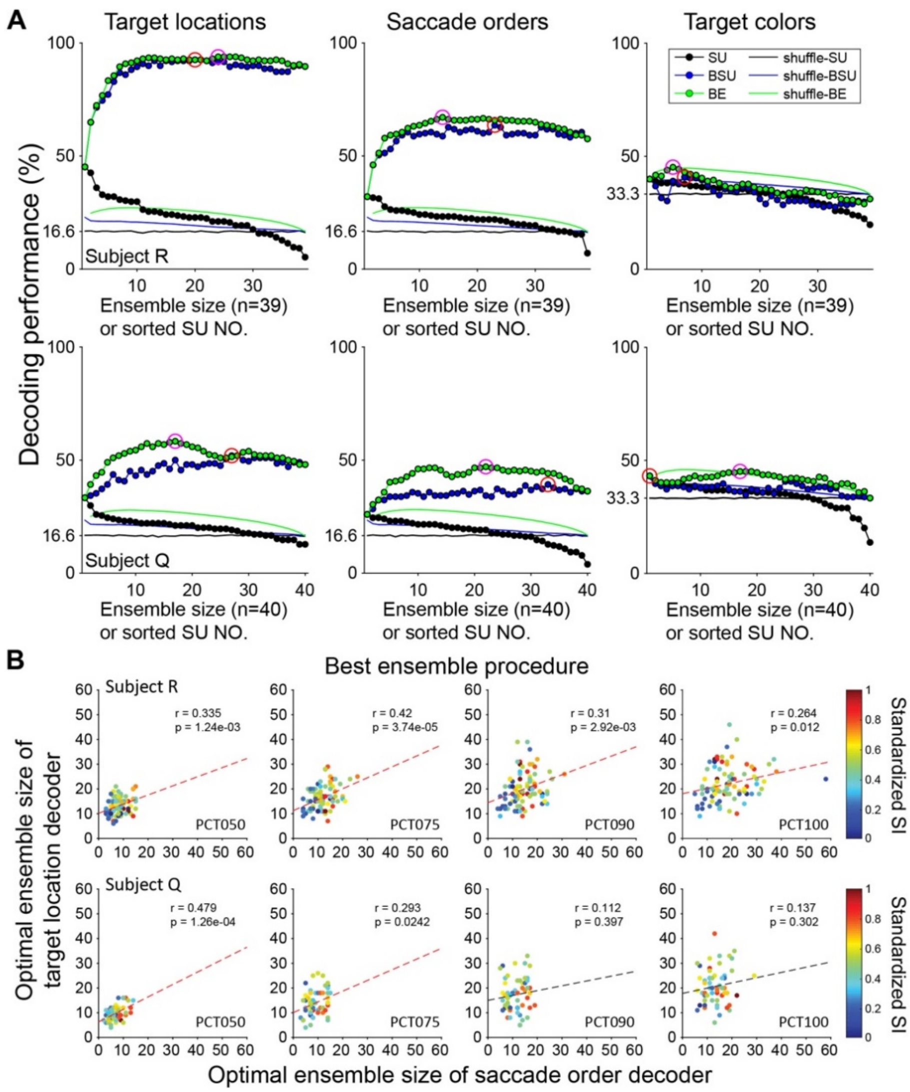

Supplemental Figure S7. Related to Figure 6. Procedures of optimal ensemble sizes. (A) Performance of target location, saccade order, and target color decoders from subject R (top) and Q (bottom) in example blocks. Black symbols show ordered single-unit decoders. Filled circles show BSU (Blue) and BE (Green) accuracies as neurons are added to the ensemble. Red and magenta circles indicated the ensemble size with maximum decoding accuracies for each approach. The same procedures were also used on shuffled data sets (BSU in blue, BE in green, and single unit in black lines). Note that BSU and BE procedures selected ensembles optimized to decode real or shuffled data, so that shuffled data accuracies are slightly above theoretical chance levels as observed in other studies (Backen et al., 2018; Leavitt et al., 2017). The chance level for target location and saccade order decoders was 16.6%, and for target color decoder was 33.3%. Compared to the BSU, BE produced higher maximum performance in the target decoders [t-test, t_{89} = 18.96, $p < 0.001$ for subject R; t_{58} = 16.91, $p < 0.001$ for subject Q], saccade order decoders [t_{89} = 20.77, $p < 0.001$ for subject R; t_{58} = 15.00, $p < 0.001$ for subject Q], and target color decoders [t_{89} = 13.40, $p < 0.001$ for subject R; t_{58} = 13.58, $p < 0.001$ for subject Q]. (B) Optimal ensemble sizes for target location and saccade order decoders were positively correlated at all percentile accuracies (PCT) for subject R, and at PCT50 and PCT75 for subject Q. There were positive correlations between the ensemble size of target and saccade decoders for all four PCT levels for subject R, but only PCT50, PCT75 for subject Q [Pearson correlation, $p < 0.05$], and larger ensemble sizes were consistently found in higher SI blocks. Each point is a trial block, color coded according to SI.